SUPPORTING INFORMATION

Carbohydrates as new probes for the identification of closely-related *E. coli* strains using surface plasmon resonance imaging

Emilie Bulard[1,2,3,4,5], Aurélie Bouchet-Spinelli[1,2,3]*, Patricia Chaud[4,5], André Roget[1,2,3], Roberto Calemczuk[1,2,3], Sébastien Fort[4,5], Thierry Livache[1,2,3]

[1]Univ. Grenoble Alpes, INAC-SPrAM-CREAB, F-38000 Grenoble, France
[2]CNRS, SPrAM-CREAB, F-38000 Grenoble, France
[3]CEA, INAC-SPrAM-CREAB, F-38000 Grenoble, France
[4]Univ. Grenoble Alpes, CERMAV, F-38000 Grenoble, France
[5]CNRS, CERMAV, F-38000 Grenoble, France

Table of Contents:

1-Preparation of allyl glycosides – supporting references

Allyl glycosides have been prepared as reported in the literature

- allyl β-D-glucopyranoside and allyl β-D-galactopyranoside from Lin, Y-Y.A.; Chalker, J.M.; Davis, B.G. *J. Am. Chem. Soc.* **2010**, *132(47)*, 16805-16811.
- allyl α-D-mannopyranoside from Nishida, Y.; Mizuno, A.; Kato, H.; Yashiro, A.; Ohtake, T.; Kobayashi, K. *Chem. Biodivers.* **2004**, *1*, 1452-1464.
- allyl β-maltoside from Takeo, T.; Imai, T. *Carbohyd. Res.* **1987**, *165(1)*, 123-128.
- allyl α-D-fucopyranoside from Vermeer, H.J.; van Dijk, C.M.; Kamerling, J.P.; Vliegenthart, J.F.G. *Eur. J. Org. Chem.* **2001**, *1*, 193-203.
- allyl α-D-N-acetyl-neuraminic acid from Roy, R.; Laferriere, C.A. *Can. J. Chem.* **1990**, *68*, 2045-2054.
- allyl 2-acetamido-2-deoxy-beta-D-glucopyranoside from Vauzeilles, B.; Dausse, B.; Palmier, S.; Beau, J-M. *Tetrahedron Lett.* **2001**, *42*, 7567-7570.

2-Characterization of pyrrole-carbohydrate conjugates

All final products were characterized by ^{1}H, ^{13}C NMR in D_2O at 25°C, 400Hz and mass spectrometry.

Pyrrole-glucose conjugate

^{1}H NMR (D_2O) δ(ppm): 6.87 (s, 2H), 6.2 (s, 2H), 4.47 (d, 1H, J=8 Hz), 4.05-3.95 (m, 4H), 3.85-3.70 (m, 2H), 3.53-3.36 (m, 5H), 3.29 (t, 1H, J=8 Hz), 2.76-2.69 (m, 4H), 2.25 (t, 2H, J=7.2 Hz), 2.11 (qt, 2H, J=6.85 Hz), 1.94 (qt, 2H, J=6.75Hz)

^{13}C NMR δ(ppm): 175.9, 121.5 (2C), 107.6 (2C), 102.3, 75.9, 73.1, 69.7, 68.8, 60.8, 48.1, 38.5, 32.7, 32.8, 30.5, 28.8, 27.4, 27.0

MS (ESI+): *m/z* = 433.1 $[M+H]^+$

Pyrrole-galactose conjugate

^{1}H NMR (D_2O) δ(ppm): 6.85 (s, 2H), 6.20 (s, 2H), 4.39 (d, 1H, J=8 Hz), 4.04-3.93 (m, 5H), 3.80-3.74 (m, 3H), 3.7-3.63 (m, 2H), 3.52 (t, 1H, J=8Hz), 3.22 (q, 1H, J=7.32 Hz), 2.74-2.68 (m, 4H), 2.25 (t, 2H, J=7.58 Hz), 2.11-2.04 (m, 2H), 1.93 (qt, 2H, J=6.75 Hz)

^{13}C NMR (D_2O) δ(ppm): 175.9, 121.5 (2C), 107.6 (2C), 102.9, 75.1, 72.8, 70.8, 68.8, 68.6, 60.9, 48.1, 38.5, 32.7, 30.5, 28.8, 27.4, 27.0

MS (ESI+): *m/z* = 433.1 $[M+H]^+$

Pyrrole-mannose conjugate

^{1}H NMR (D_2O) δ(ppm): 6.86 (s, 2H), 6.22 (s, 2H), 4.9 (s, 1H), 4.04-3.60 (m, 10H), 3.41 (t, 2H, J=6.52Hz), 2.75-2.67 (m, 4H), 2.25 (t, 2H, J=7.26 Hz), 2.12-2.04 (m, 2H), 1.93 (qt, 2H, J=6.3 Hz)

^{13}C NMR (D_2O) δ(ppm): 175.9, 121.5 (2C), 107.6 (2C), 99.7, 72.8, 70.6, 70.1, 66.7, 66.1, 60.9, 48.1, 38.5, 32.8, 30.5, 28.5, 27.8, 27.0

MS (ESI+): *m/z* = 433.1 $[M+H]^+$

Pyrrole-fucose conjugate

^{1}H NMR (D_2O) δ(ppm): 6.86 (s, 2H), 6.22 (s, 2H), 4.9 (d, 1H, J=3.84 Hz), 4.07 (q, 1H, J=6.59 Hz), 4.02-4.0 (m, 2H), 3.99-3.78 (m, 4H), 3.62-3.57 (m, 1H), 3.41 (t, 2H, J=6.54 Hz), 2.75-2.69 (m, 4H), 2.24 (t, 2H, J=7.28 Hz), 2.09 (qt, 2H, J=7.04 Hz), 2-1.89 (m, 2H), 1.24 (d, 3H, J=6.64Hz)

^{13}C NMR (D_2O) δ(ppm): 175.8, 121.5 (2C), 107.6 (2C), 98.4, 71.8, 69.6, 68.0, 66.6, 66.5, 48.1, 38.5, 32.8, 30.5, 28.6, 27.8, 27.0, 15.3

MS (ESI+): *m/z* = 417.1 $[M+H]^+$

Pyrrole-maltose conjugate

^{1}H NMR (D_2O) δ(ppm): 6.87 (s, 2H), 6.22 (s, 2H), 5.42 (d, 1H, J=3.8 Hz), 4.48 (d, 1H, J=8Hz), 4.04-3.41 (m, 18H), 3.32 (t, 1H, J=8.72 Hz), 2.75-2.69 (m, 4H), 2.25 (t, 2H, J=7.26 Hz), 2.09 (qt, 2H, J=6.81 Hz), 1.94 (qt, 2H, J=6.72 Hz)

^{13}C NMR (D_2O) δ(ppm): 175.9, 121.5 (2C), 107.6 (2C), 102.2, 99.6, 76.9, 76.2, 74.6, 73.0, 72.9, 72.7, 71.7, 69.3, 68.8, 60.7, 60.5, 48.1, 38.5, 32.7, 30.5, 28.8, 27.4, 27.0

MS (ESI+): *m/z* = 595.1 $[M+H]^+$

Pyrrole-(*N*-acetyl-glucosamine) conjugate

^{1}H NMR (D_2O) δ(ppm): 6.87 (s, 2H), 6.22 (s, 2H), 4.51 (d, 1H, J=8.4Hz), 4.02-3.44 (m, 10H), 3.40 (t, 2H, J=6.52 Hz), 2.71-2.59 (m, 4H), 2.31-2.22 (m, 2H), 2.12-2.04 (m, 5H), 1.92-1.82 (m, 2H)

^{13}C NMR (D_2O) δ(ppm): 175.9, 174.4, 121.5 (2C), 107.6 (2C), 101.2, 75.9, 73.8, 70.0, 68.6, 60.7, 55.6, 48.1, 38.5, 32.7, 30.5, 28.6, 27.4, 27.0, 22.3
MS (ESI+): *m/z* = 474.1 $[M+H]^+$

Pyrrole-sialic acid conjugate

^{1}H NMR (D_2O) δ(ppm): 6.87 (s, 2H), 6.22 (s, 2H), 3.99 (t, 2H, J=6.7Hz), 3.94-3.54 (m, 9H), 3.40 (t, 2H, J= 6.5 Hz), 3.23* (q, 6H, J=7.3 Hz), 2.79-2.64 (m, 5H), 2.25 (t, 2H, J=7.26 Hz), 2.12-2.07 (m, 5H), 1.87 (qt, 2H, J=6.75 Hz), 1.68 (t, 1H, J=12.1Hz), 1.31* (t, 9H, J= 7.32 Hz
^{13}C NMR (D_2O) δ(ppm): 175.9, 175.1, 173.6, 121.5 (2C), 107.6 (2C), 100.6, 72.6, 71.8, 68.3, 62.8, 63.3, 62.6, 51.9, 48.1, 46.7*, 40.4, 38.5, 32.7, 30.4, 29.1, 27.6, 27.0, 22.0, 8.2*
* Signals of triethylammonium counterion
MS (ESI-): *m/z* = 560.1 $[M-Et_3NH]^-$

3-SPRi data treatment

SPRi signals of the bacterial growth onto the carbohydrate microarray were represented by an inverse tangent function: after smoothing kinetic curves, first order derivative of this function was realized (Figure S-1). The maximum of the derivative corresponds to the inflection point of kinetic curve called "detection time". Thus, "detection time" of distinguished and control SPRi signal were measured and the "differential time" was obtained by subtracting these two times.

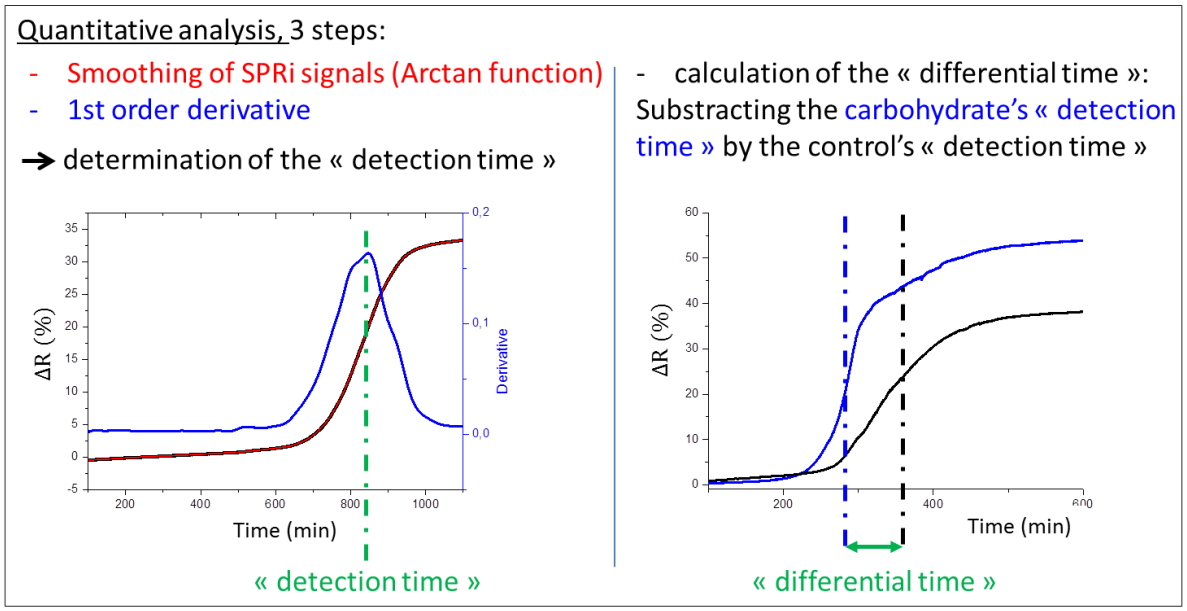

Figure S-1. Detection time and differential time calculations.

4-Contribution of one bacterium to the SPRi signal

SPRi plots reflect the global change of the refractive index in the medium which results from the presence of bacteria 100-300 nm above the gold surface (*i.e* length of the evanescent wave interacting with the gold surface plasmon). Then, the reflectivity amplitudes depend on the contribution of one bacterium to the SPRi signal (Figure S-2). If bacteria interact through their flagella, the contribution of one bacterium to the SPRi signal will be poor since the evanescent wave will probe only ~1% of the flagella' s length. On the contrary, if bacteria interact through their pili or core bacterial surface receptors, more of the "mass" of one bacterium will be probed by the evanescent wave. Then, the contribution to the SPRi signal will be more important (*i.e* ΔR will increase).

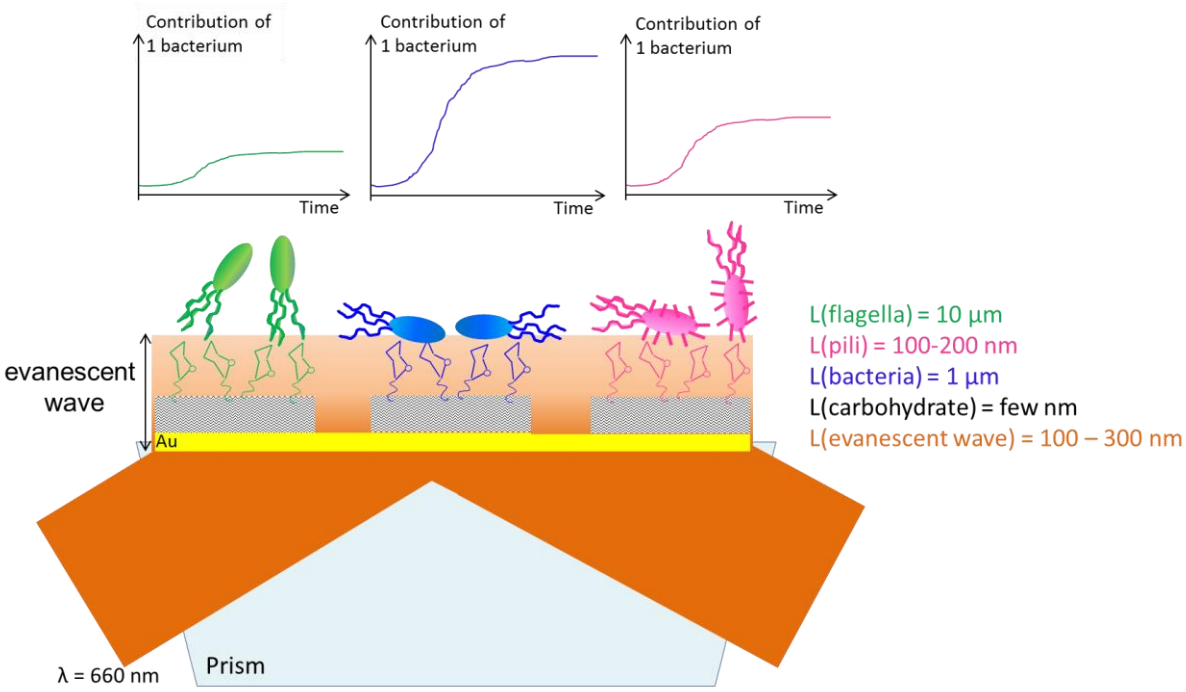

Figure S-2. Contribution of bacteria to the SPRi signal. The graph is not to scale.

5-Influence of the carbohydrate density onto the microarray towards carbohydrate-bacteria interactions

All the SPRi experiments described in this article were realized with copolymer spots with initial formulations of 20mM pyrrole and 10mM pyrrole-carbohydrate conjugates. The same experiments were also realized with 100µM (Figure S-3) and 2mM (not shown) pyrrole-carbohydrate conjugates concentrations using the same protocols.

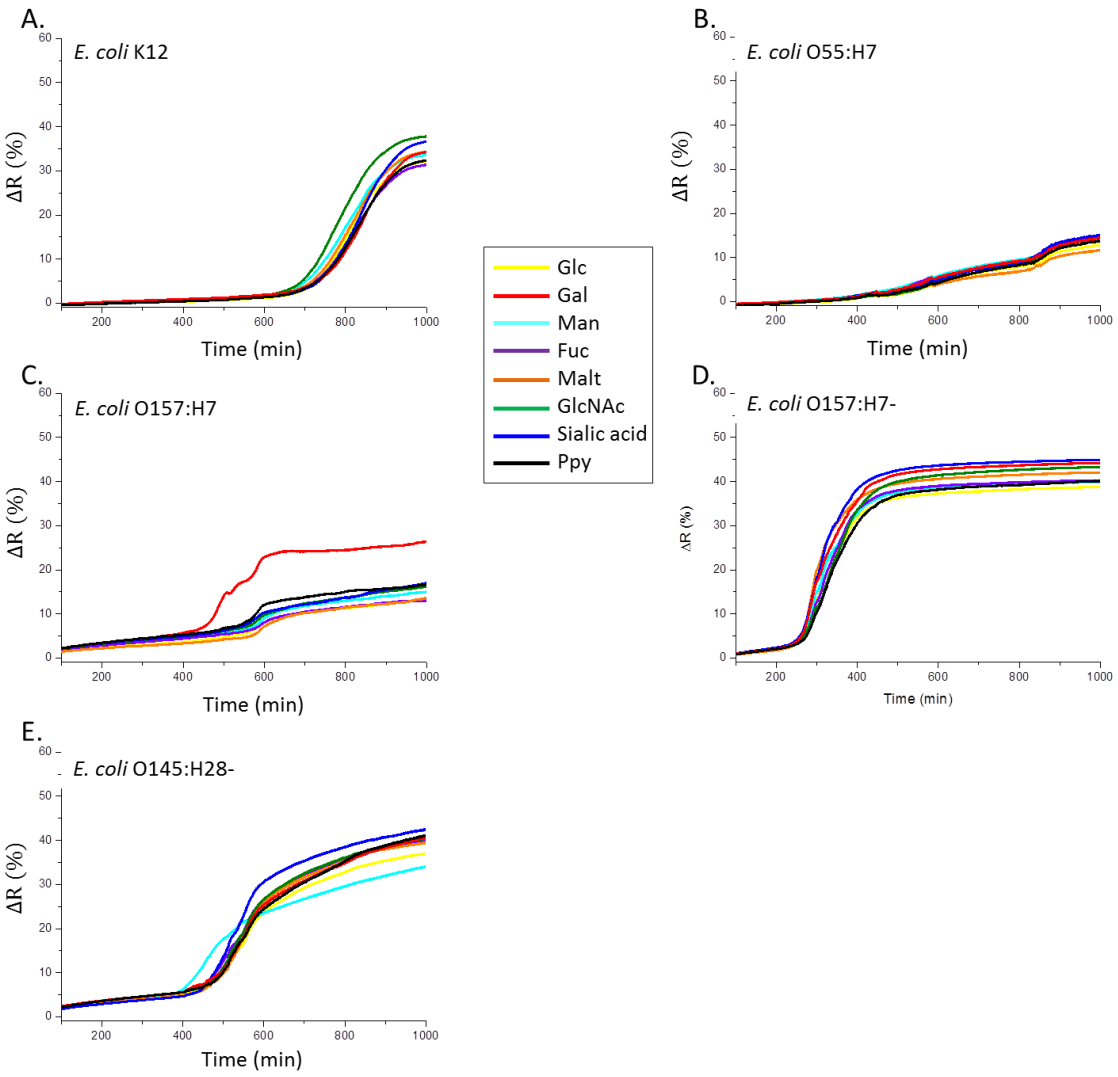

Figure S-3. SPRi signals obtained from the biochip conceived using the formulation 20mM pyrrole/100 µM pyrrole-carbohydrate conjugates, after deposition of the bacterial suspension at 10^2 CFU.mL^{-1} in TSB; in the case of: A. *E. coli* K12, B. *E. coli* O55:H7, C. *E. coli* O157:H7, D. *E. coli* O157:H7$^-$, E. *E. coli* O145:H28$^-$.

The same data treatment was applied (see Experimental section) and results are summarized in Table S-1. "Detection times" of the different bacterial strains did not depend on the density of sugars in the copolymer. But, the "differential time", reflecting the difference between the detection times of a distinguished carbohydrate and the control (polypyrrole), increased from the 100µM pyrrole-carbohydrate conjugate formulation. Indeed, at the 100 µM formulation, only galactose interacting with *E. coli* O157:H7 and mannose, galactose interacting with *E. coli* O145:H28$^-$ were observed (Figure S-2 C. and E.). The positivity criterion was reached for *E. coli* O157:H7$^-$ for a pyrrole-carbohydrate conjugate formulation at 10mM. These results are probably due to effects of multivalency in protein-carbohydrate recognition.

Thus, the biochip for greater discrimination between all the different bacterial strains and carbohydrates was that of 10mM.

Bacterial strains	*E. coli* K12	*E. coli* O157:H7	*E. coli* O157:H7⁻	*E. coli* O55:H7	*E. coli* O145:H28⁻		
Interacting carbohydrate	Any sugars	Galactose	Sialic acid	Any sugars	Mannose	Galactose	Sialic acid
Formulation at 20mM pyrrole/100µM pyrrole-carbohydrate conjugate							
Detection time (min)	829 ± 5	549 ± 43	326 ± 19	872 ± 9	456 ± 6	507 ± 35	518 ± 4
Differential time (min)	Ø	57 ± 53	Ø	Ø	68 ± 35	24 ± 23	Ø
Formulation at 20mM pyrrole/2mM pyrrole-carbohydrate conjugate							
Detection time (min)	829 ± 5	516 ± 28	328 ± 22	872 ± 9	449 ± 6	470 ± 27	483 ± 27
Differential time (min)	Ø	94 ± 29	Ø	Ø	74 ± 29	53 ± 31	40 ± 31
Formulation at 20mM pyrrole/10mM pyrrole-carbohydrate conjugate							
Detection time (min)	829 ± 5	529 ± 26	295 ± 7	872 ± 9	448 ± 8	473 ± 4	494 ± 21
Differential time (min)	Ø	76 ± 32	47 ± 20	Ø	78 ± 15	53 ± 11	32 ± 17

Table S-1. Detection time and differential time between distinguished curves and the other ones at the inflection point of SPR signals obtained from the spots made with 100µm – 2mM – 10mM of pyrrole-carbohydrate conjugates in the initial copolymer formulation, after deposition of the bacterial suspension at 10^2 CFU.mL^{-1} in TSB. Data were obtained from the SPRi signal averages of three independent runs.

6-Influence of the initial bacterial concentration

All the SPRi experiments described in the manuscript were realized with an initial bacterial concentration of 10^2 CFU.mL^{-1}. We have also realized the same SPRi experiment on the biochip with an initial *E. coli* O157:H7 concentration of 10^4 CFU.mL^{-1} (Figure S-4). The detection time of *E. coli* O157:H7/galactose interaction goes logically down to the value of 364 min and the detection times of the interaction of this bacterium with the other carbohydrates go also down (463 ± 8 min). Thus, the time difference between the earlier interaction of *E. coli* O157:H7 with galactose and the controls remain the same for initial concentrations of 10^2 CFU.mL^{-1} and 10^4 CFU.mL^{-1}.

As a conclusion, the time difference criterion that we chose is the most relevant since it seems not to depend on the initial bacterial concentration.

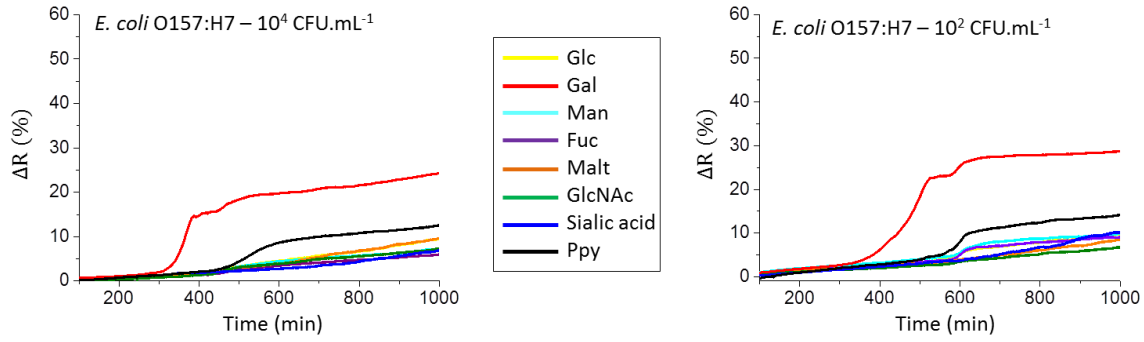

Figure S-4. SPRi signals obtained from the biochip conceived using the formulation 20mM pyrrole/10 mM pyrrole-carbohydrate conjugates, after deposition of the bacterial suspension of *E. coli* O157:H7 at 10^4 CFU.mL^{-1} (left) and at 10^2 CFU.mL^{-1} (right) in TSB.